JACS
JOURNAL OF THE AMERICAN CHEMICAL SOCIETY
pubs.acs.org/JACS
Communication

Label-Free Digital Detection of Intact Virions by Enhanced Scattering Microscopy

Nantao Li,[▽] Xiaojing Wang,[▽] Joseph Tibbs,[▽] Congnyu Che, Ana Sol Peinetti, Bin Zhao, Leyang Liu, Priyash Barya, Laura Cooper, Lijun Rong, Xing Wang, Yi Lu,* and Brian T. Cunningham*

Cite This: https://doi.org/10.1021/jacs.1c09579

ABSTRACT: Several applications in health diagnostics, food, safety, and environmental monitoring require rapid, simple, selective, and quantitatively accurate viral load monitoring. Here, we introduce the first label-free biosensing method that rapidly detects and quantifies intact virus in human saliva with single-virion resolution. Using pseudotype SARS-CoV-2 as a representative target, we immobilize aptamers with the ability to differentiate active from inactive virions on a photonic crystal, where the virions are captured through affinity with the spike protein displayed on the outer surface. Once captured, the intrinsic scattering of the virions is amplified and detected through interferometric imaging. Our approach analyzes the motion trajectory of each captured virion, enabling highly selective recognition against nontarget virions, while providing a limit of detection of 1×10^3 copies/mL at room temperature. The approach offers an alternative to enzymatic amplification assays for point-of-collection diagnostics.

Most assays for the detection of viral pathogens target either the surface proteins or nucleic acids. The most widely adopted diagnostic methods, based upon nucleic acid amplification by the polymerase chain reaction (PCR), use nucleic acid primers to detect the presence of the viral genome in bodily fluids. Although highly sensitive, PCR tests suffer from a complex assay workflow that requires enzymes, thermal cycles, virus lysis, and nucleic acid extraction that contribute to their high cost and extended time between sample collection and result.[1] Alternatively, by directly detecting proteins originating from the virus outer shell, antigen-based assays greatly reduce turnaround time but with much reduced sensitivity, and often require additional labels (such as quantum dots,[2] gold nanoparticles,[3] and other labels[4]) to enhance the signal contrast.

The COVID-19 pandemic is among the most significant and severe global health events in the modern era, and mass screening is a crucial measure to reduce SARS-CoV-2 transmission. However, the rapid surge of tests leads to supply shortage of reagents for conventional tests such as primers and fluorophores. More importantly, there is no existing detection technique that can determine the infectivity of SARS-CoV-2, which is critical to reduce and prevent false diagnoses, as it is reported that for some patients residual viral RNA remains detectable even though no viable SARS-CoV-2 can be observed by culture.[5]

Recently developed label-free biodetection technologies show great promise as the next generation of clinical diagnostic tools, allowing for simple, cost-effective yet highly sensitive virus detection. Exploiting the enhanced sensitivity of nanostructured electrodes[6] and graphene-based field-effect transistors,[7] semiconductor-based electrochemical sensors demonstrated on-demand viral level determination for SARS-CoV-2, without extrinsic labels or elaborate procedures. Recent advances in nanophotonic/plasmonic resonating structures have also demonstrated an unprecedented ability to observe and detect molecular interactions with single-molecule resolution. Facilitated by the enhanced light−matter interaction via surface plasmon resonance[8] or high-quality resonators,[9] the presence of single viruses can induce changes in the resonance frequency or mode splitting which are used as the signal readout. However, these techniques are often limited to making ensemble measurements where the combined effects of many virions are averaged to a single electrical or optical signal, with the background noise greatly limiting the sensitivity.[10]

In response to the limitations of the current COVID-19 diagnostic techniques, we present a label-free sensing method for intact SARS-CoV-2 viral particles with single-virus resolution. As shown in Figure 1a, the nanophotonic biosensor consists of two parts: a photonic crystal (PC), which is a corrugated dielectric resonator that functions as the transducer substrate, and DNA aptamer immobilized ligands, covalently attached to the PC surface. As reported recently, the PC enables an amplified interferometric scattering imaging modality through the photonic band edge effect, allowing the direct detection of individual viruses and protein molecules by their elastic scattering signal.[11] This label-free imaging technique, called photonic resonator interferometric scattering microscopy (PRISM), offers enhanced near-field excitation by light confinement (Figure 1b,c) and permits real-time visualization and mass quantification of virions near the PC surface.

Received: September 9, 2021

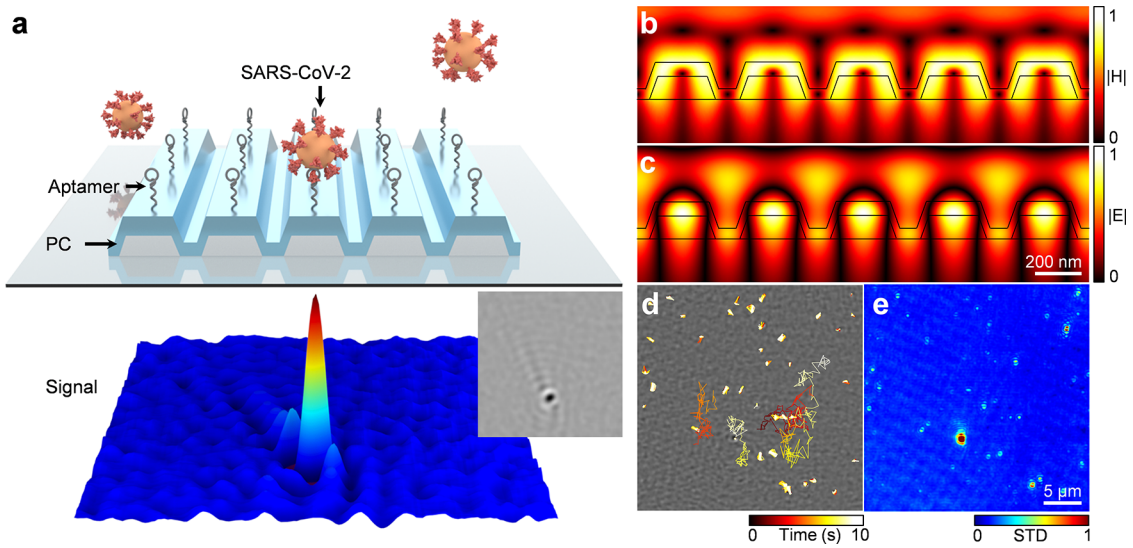

Figure 1. Working principle of label-free optical detection for intact SARS-CoV-2. (a) Schematics of the label-free optical biosensor design, in which DNA aptamers are immobilized on the PC surface by epoxysilane-based covalent chemistry. The elastically scattered light from any viral particles near the surface will be enhanced and detected by PC via interferometric scattering imaging. Inset: Exemplary interferometric image of a single SARS-CoV-2 virion. (b,c) Distribution of magnetic and electric field of the PC under the resonant condition. (d) Lateral trajectories of viral particles on the aptamer-decorated PC surface. (e) Image of temporal standard deviation for the visualization of captured virions.

Although the label-free visualization of virions has been demonstrated in other interferometric scattering microscopy platforms,[12] here we integrate the highly selective DNA aptamers with PRISM to directly monitor the kinetics of each viral particle and their interaction with the surface-conjugated aptamers, thus establishing the presence of SARS-CoV-2 with high specificity for active virions and digital-resolution sensitivity.

Featuring flexibility, stability, cost effectiveness, and simplicity in production, DNA aptamers with specific 3D conformation can recognize their target molecules with a high binding affinity rivaling that of antibodies. To identify aptamer sequences for SARS-CoV-2 virion recognition, we performed a combinatorial selection process called systematic evolution of ligands by exponential enrichment (SELEX)[13] with pseudotyped SARS-CoV-2 (p-SARS-CoV-2) virions as the target. Unlike wild-type SARS-CoV-2, which is classified as a Biosafety Level 3 (BSL-3) agent, p-SARS-CoV-2 virions derived from lentiviral vectors have been extensively used to create virions with desirable surface structures and specific envelope-presented proteins.[14] Effectively, the spike (S) proteins of SARS-CoV-2 is decorated on the envelope surface of a lentivirus which maintains the architecture of the virion but is limited to a single cycle of viral infection, rendering it a BSL-2 agent. Although defective in continuous replication, the pseudotyped viruses maintain the native structure of SARS-CoV-2 on the viral surface and mediate entry of the viruses to the host cell, thus providing a safe and ideal model for assay development in BSL-2 facilities. To promote the selectivity of the final aptamer probes, several interfering species were incorporated in the SELEX counter selection step: UV-inactivated p-SARS-CoV-2, whose surface proteins and genome content are damaged, was used to obtain selectivity for active p-SARS-CoV-2; other types of pseudotyped viruses (SARS-CoV and H5N1) were also used to prevent potential cross-reactivity (see Supporting Information for all methods and materials). A 45-mer sequence was identified from the SELEX process and named SARS2-AR10, with K_d = 79 ± 28 nM.[15]

To characterize the performance of SARS2-AR10 on PRISM, we first exposed the aptamer-conjugated PC to a high concentration (1×10^9 copies/mL) of p-SARS-CoV-2. Within the 10 s observation window (Supplemental Video 1), we can individually track the trajectories of virions near the PC surface (Figure 1d), of which the majority remained locally confined due to the aptamer−virus interaction in contrast to the few which were not bound to any aptamer and underwent Brownian motion. By performing pixel-wise temporal standard deviation (Figure 1e), the signal from each confined virion can be clearly distinguished and respectively numerated as the gauge for SARS-CoV-2 viral level. The kinetics of the label-free biosensor was obtained by recording the surface density of the captured virions as a function of incubation time at a 30 min interval for up to 2 h (Figure 2a). Although significant surface density of p-SARS-CoV-2 could be observed within 5 min, we extended the incubation time for up to 2 h to provide quantitation over a broad dynamic range. In addition, we compared the performance of SARS2-AR10 with other reported aptamers targeting the S protein[16] or its receptor binding domain (RBD)[17] on SARS-CoV-2 (Supplemental Figure 1). Under the same conditions, SARS2-AR10 demonstrated significantly higher capturing efficiency against intact viruses than the control sequences.

The dose−response characteristic of our approach was obtained by quantifying the surface density of the surface-captured virions as a function of concentration for serially diluted p-SARS-CoV-2 (Figure 2b,c). For viral concentration as low as 1×10^3 copies/mL, we observed signal clearly distinguishable from that of the blank control. Further reduction in viral concentration leads to insufficient virus count limited by sample volume and background interference. By combining aptamer molecules with PC biosensors and PRISM, sensitivity commensurate with PCR and other enzymatic amplification based techniques[18] can be achieved at a fraction of the cost (Supplemental Table 1). The

https://doi.org/10.1021/jacs.1c09579
J. Am. Chem. Soc. XXXX, XXX, XXX−XXX

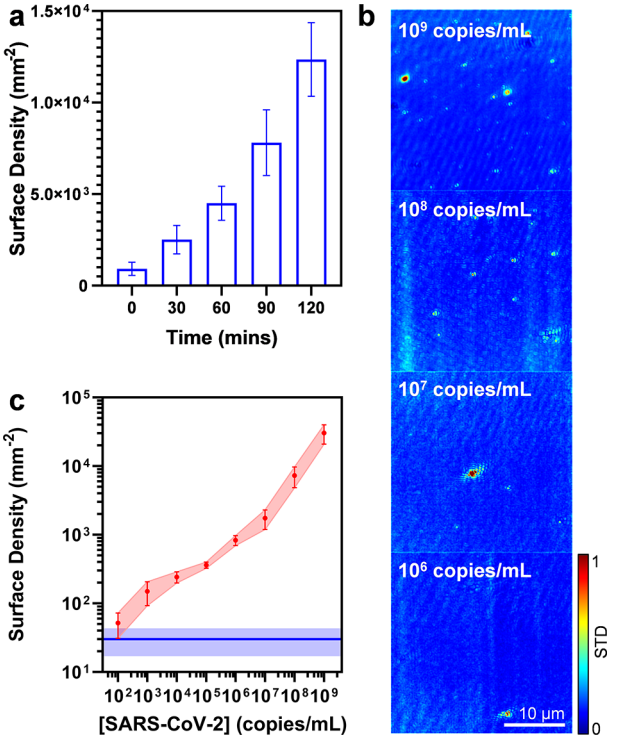

Figure 2. Dose response of SARS2-AR10 based single-virus detection. (a) Time-dependent surface density in the presence of pseudotyped SARS-CoV-2 (1×10^9 copies/mL). Within 5 min of incubation, significant signal can be observed. (b) Representative temporal standard deviation images of captured p-SARS-CoV-2 at various concentrations with 2-h incubation. (c) Surface density quantification of captured virions as the dose response curve. Negative control (blue baseline) contains only buffer solution. Error bars represent the standard deviations of three independent measurements.

specificity of the assay was examined by introducing other common viruses as the interfering species, such as 229E coronavirus (responsible for the common cold), pseudotyped H5N1 influenza virus, pseudotyped SARS-CoV, and UV-inactivated p-SARS-CoV-2, all of which share a similar size (hydrodynamic radius of approximately 50 nm) as validated by the volume-dependent contrast signal by PRISM (Figure 3a). The contrast values of these viruses are approximately 1 order of magnitude higher than the background noise. At the same concentration, statistically significant reduction in virus surface capture density was observed for all the interfering viruses, indicating outstanding specificity for active p-SARS-CoV-2 and minimal cross-reactivity even for SARS-CoV (Figure 3b).

To explore the feasibility of the label-free nanophotonic sensor in clinical applications, we further challenged the assay with crude saliva spiked with p-SARS-CoV-2 viruses. In comparison with invasive nasopharyngeal swabbing, saliva-based COVID-19 diagnosis benefits from a less invasive sample collection procedure and has promising potential in mass screening. Spiked specimens were passed through syringe filters (pore size 0.2 μm) to remove particulate matter larger than the virus present in crude saliva. Prior to imaging, the sample was rinsed with buffer solution to remove nonspecific bindings. The results indicate that our approach maintains a similar level of sensitivity and selectivity despite the complex media, reaching a detection limit of 5×10^3 copies/mL in saliva (Figure 3c).

In summary, we have described a label-free SARS-CoV-2 detection approach with single-virus resolution with sensitivity commensurate with that of the PCR technique. By virtue of the lab-screened aptamer as the recognition element, active SARS-CoV-2 pseudoviruses were differentiated with statistical significance from their inactive counterparts and other interfering common viruses including SARS-CoV. Compared with other emerging SARS-CoV-2 detection techniques,[6,7,18] our aptamer-PRISM platform is the first label-free biosensing method with the capability of detecting individual viral particles in human saliva. The wide dynamic range (5×10^3 to 1×10^9 copies/mL) in the spike-in saliva test covers the viral load level of SARS-CoV-2 (1×10^4 to 1×10^7 copies/mL) at the early stage of infection.[19] Regarding the detection limit, in comparison with other detection techniques like PCR (3×10^3 copies/mL[18]) and LAMP (5×10^4 copies/mL[20]), our approach achieves a similar performance but with the capability of individually detecting intact virions without the need for lysis and nucleic acid extraction, thus greatly reducing the overall cost and procedural complexity. We anticipate that the incubation time can be further reduced by the incorporation of a simple microfluidic device, which would improve the kinetics of viral binding to the sensor surface. By leveraging the versatility of DNA aptamers and the SELEX

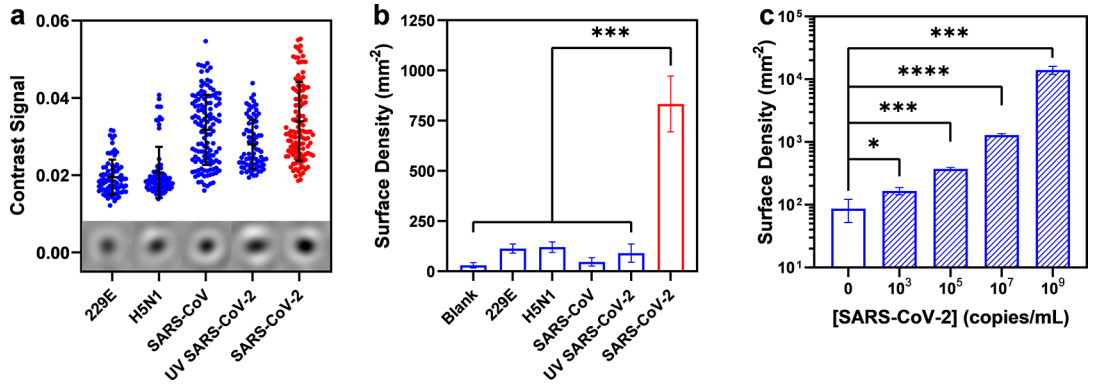

Figure 3. Selectivity for active SARS-CoV-2 and analysis of human saliva sample. (a) Contrast distribution of each type of virus for size characterization. Each dot represents the interferometric contrast signal from one viral particle. (b) Specificity test for viral detection based on SARS2-AR10. All viruses used were at a concentration of 1×10^6 copies/mL. (c) Sensor performance in human saliva. For spiked-in sample, SARS-CoV-2 concentration was adjusted to various concentrations with crude human saliva pooled from healthy subjects. Error bars represent the standard deviations of at least three independent measurements.

https://doi.org/10.1021/jacs.1c09579
J. Am. Chem. Soc. XXXX, XXX, XXX−XXX

process for aptamer screening, we envision that this detection technique can be easily and rapidly extended to monitor other viruses and prepare for future epidemics and pandemics.

■ ASSOCIATED CONTENT

Supporting Information

The Supporting Information is available free of charge at https://pubs.acs.org/doi/10.1021/jacs.1c09579.

Procedure for PC fabrication, characterization, and functionalization; details of pseudotyped virus preparation and quantification; SELEX process for virus-specific aptamer selection; procedure for human saliva spike-in test; instrumentation and data analysis for PRISM system; numerical analysis of the PC under resonant condition and the corresponding interferometric scattering image; tables of cost estimates, DNA sequences, and pseudovirus titration; figures of sensitivity of DNA aptamers, FIB-SEM image, TEM characterization, SELEX process, and simulated PRISM images (PDF)

Exemplary video of SARS-CoV-2 detected by PRISM (MP4)

■ AUTHOR INFORMATION

Corresponding Authors

Yi Lu − *Department of Chemistry, Department of Bioengineering, and Carl R. Woese Institute for Genomic Biology, University of Illinois at Urbana−Champaign, Urbana, Illinois 61801, United States;* orcid.org/0000-0003-1221-6709; Email: yi-lu@illinois.edu

Brian T. Cunningham − *Department of Electrical and Computer Engineering, University of Illinois at Urbana−Champaign, Urbana, Illinois 61801, United States; Nick Holonyak Jr. Micro and Nanotechnology Laboratory, Department of Bioengineering, Carl R. Woese Institute for Genomic Biology, and Cancer Center at Illinois, University of Illinois at Urbana−Champaign, Urbana, Illinois 61801, United States*; Email: bcunning@illinois.edu

Authors

Nantao Li − *Department of Electrical and Computer Engineering, University of Illinois at Urbana−Champaign, Urbana, Illinois 61801, United States; Nick Holonyak Jr. Micro and Nanotechnology Laboratory, University of Illinois at Urbana−Champaign, Urbana, Illinois 61801, United States;* orcid.org/0000-0003-2541-3445

Xiaojing Wang − *Nick Holonyak Jr. Micro and Nanotechnology Laboratory and Department of Chemistry, University of Illinois at Urbana−Champaign, Urbana, Illinois 61801, United States*

Joseph Tibbs − *Nick Holonyak Jr. Micro and Nanotechnology Laboratory and Department of Bioengineering, University of Illinois at Urbana−Champaign, Urbana, Illinois 61801, United States*

Congnyu Che − *Nick Holonyak Jr. Micro and Nanotechnology Laboratory and Department of Bioengineering, University of Illinois at Urbana−Champaign, Urbana, Illinois 61801, United States;* orcid.org/0000-0002-8224-0803

Ana Sol Peinetti − *Department of Chemistry, University of Illinois at Urbana−Champaign, Urbana, Illinois 61801, United States;* orcid.org/0000-0002-9304-3004

Bin Zhao − *Nick Holonyak Jr. Micro and Nanotechnology Laboratory and Carl R. Woese Institute for Genomic Biology, University of Illinois at Urbana−Champaign, Urbana, Illinois 61801, United States;* orcid.org/0000-0002-0987-4586

Leyang Liu − *Department of Electrical and Computer Engineering, University of Illinois at Urbana−Champaign, Urbana, Illinois 61801, United States; Nick Holonyak Jr. Micro and Nanotechnology Laboratory, University of Illinois at Urbana−Champaign, Urbana, Illinois 61801, United States*

Priyash Barya − *Department of Electrical and Computer Engineering, University of Illinois at Urbana−Champaign, Urbana, Illinois 61801, United States; Nick Holonyak Jr. Micro and Nanotechnology Laboratory, University of Illinois at Urbana−Champaign, Urbana, Illinois 61801, United States*

Laura Cooper − *Department of Microbiology and Immunology, College of Medicine, University of Illinois at Chicago, Chicago, Illinois 60612, United States*

Lijun Rong − *Department of Microbiology and Immunology, College of Medicine, University of Illinois at Chicago, Chicago, Illinois 60612, United States*

Xing Wang − *Nick Holonyak Jr. Micro and Nanotechnology Laboratory, Department of Chemistry, and Carl R. Woese Institute for Genomic Biology, University of Illinois at Urbana−Champaign, Urbana, Illinois 61801, United States*

Complete contact information is available at: https://pubs.acs.org/10.1021/jacs.1c09579

Author Contributions

[▽]N.L., X.W., and J.T. contributed equally.

Notes

The authors declare no competing financial interest.

■ ACKNOWLEDGMENTS

This work was supported by National Institutes of Health (R01 CA227699-01, R01 AI159454) and National Science Foundation (NSF RAPID 20-27778, CBET 20-29215). N.L. acknowledges support from Zhejiang University ZJU-UIUC Joint Research Center (DREMES202001) and from the Mikashi award of the Carl R. Woese Institute for Genomic Biology. The authors thank Prof. Thomas Gallagher at Loyola University Chicago for the 229E-CoV sample.

■ ABBREVIATIONS

229E, human corona virus (strain 229E); PC, photonic crystal; PRISM, photonic resonator interferometric scattering microscopy; RBD, receptor binding domain; SELEX, systematic evolution of ligands by exponential enrichment

■ REFERENCES

(1) Smyrlaki, I.; Ekman, M.; Lentini, A.; de Sousa, N. R.; Papanicolaou, N.; Vondracek, M.; Aarum, J.; Safari, H.; Muradrasoli, S.; Rothfuchs, A. G. Massive and rapid COVID-19 testing is feasible by extraction-free SARS-CoV-2 RT-PCR. *Nat. Commun.* **2020**, *11* (1), 4812.

(2) Gorshkov, K.; Susumu, K.; Chen, J.; Xu, M.; Pradhan, M.; Zhu, W.; Hu, X.; Breger, J. C.; Wolak, M.; Oh, E. Quantum dot-conjugated SARS-CoV-2 spike pseudo-virions enable tracking of angiotensin converting enzyme 2 binding and endocytosis. *ACS Nano* **2020**, *14* (9), 12234−12247.

(3) Moitra, P.; Alafeef, M.; Dighe, K.; Frieman, M. B.; Pan, D. Selective naked-eye detection of SARS-CoV-2 mediated by N gene targeted antisense oligonucleotide capped plasmonic nanoparticles. *ACS Nano* **2020**, *14* (6), 7617−7627.
(4) Deng, J.; Zhao, S.; Liu, Y.; Liu, C.; Sun, J. Nanosensors for diagnosis of infectious diseases. *ACS Appl. Bio Mater.* **2021**, *4* (5), 3863−3879.
(5) Joynt, G. M.; Wu, W. K. Understanding COVID-19: what does viral RNA load really mean? *Lancet Infect. Dis.* **2020**, *20* (6), 635−636.
(6) Yousefi, H.; Mahmud, A.; Chang, D.; Das, J.; Gomis, S.; Chen, J. B.; Wang, H.; Been, T.; Yip, L.; Coomes, E. Detection of SARS-CoV-2 viral particles using direct, reagent-free electrochemical sensing. *J. Am. Chem. Soc.* **2021**, *143* (4), 1722−1727.
(7) Seo, G.; Lee, G.; Kim, M. J.; Baek, S.-H.; Choi, M.; Ku, K. B.; Lee, C.-S.; Jun, S.; Park, D.; Kim, H. G. Rapid detection of COVID-19 causative virus (SARS-CoV-2) in human nasopharyngeal swab specimens using field-effect transistor-based biosensor. *ACS Nano* **2020**, *14* (4), 5135−5142.
(8) Yanik, A. A.; Huang, M.; Kamohara, O.; Artar, A.; Geisbert, T. W.; Connor, J. H.; Altug, H. An optofluidic nanoplasmonic biosensor for direct detection of live viruses from biological media. *Nano Lett.* **2010**, *10* (12), 4962−4969.
(9) Zhu, J.; Özdemir, Ş. K.; He, L.; Chen, D.-R.; Yang, L. Single virus and nanoparticle size spectrometry by whispering-gallery-mode microcavities. *Opt. Express* **2011**, *19* (17), 16195−16206.
(10) Taylor, A. B.; Zijlstra, P. Single-molecule plasmon sensing: current status and future prospects. *ACS Sens.* **2017**, *2* (8), 1103−1122.
(11) Li, N.; Canady, T. D.; Huang, Q.; Wang, X.; Fried, G. A.; Cunningham, B. T. Photonic resonator interferometric scattering microscopy. *Nat. Commun.* **2021**, *12* (1), 1744.
(12) (a) Kukura, P.; Ewers, H.; Müller, C.; Renn, A.; Helenius, A.; Sandoghdar, V. High-speed nanoscopic tracking of the position and orientation of a single virus. *Nat. Methods* **2009**, *6* (12), 923−927. (b) Huang, Y.-F.; Zhuo, G.-Y.; Chou, C.-Y.; Lin, C.-H.; Chang, W.; Hsieh, C.-L. Coherent brightfield microscopy provides the spatio-temporal resolution to study early stage viral infection in live cells. *ACS Nano* **2017**, *11* (3), 2575−2585. (c) Daaboul, G.; Yurt, A.; Zhang, X.; Hwang, G.; Goldberg, B.; Unlu, M. High-throughput detection and sizing of individual low-index nanoparticles and viruses for pathogen identification. *Nano Lett.* **2010**, *10* (11), 4727−4731. (d) Seymour, E.; Unlu, N. L.; Carter, E. P.; Connor, J. H.; Unlu, M. S. Configurable Digital Virus Counter on Robust Universal DNA Chips. *ACS sensors* **2021**, *6* (1), 229−237.
(13) Sefah, K.; Shangguan, D.; Xiong, X.; O'donoghue, M. B.; Tan, W. Development of DNA aptamers using Cell-SELEX. *Nat. Protoc.* **2010**, *5* (6), 1169−1185.
(14) Crawford, K. H.; Eguia, R.; Dingens, A. S.; Loes, A. N.; Malone, K. D.; Wolf, C. R.; Chu, H. Y.; Tortorici, M. A.; Veesler, D.; Murphy, M. Protocol and reagents for pseudotyping lentiviral particles with SARS-CoV-2 spike protein for neutralization assays. *Viruses* **2020**, *12* (5), 513.
(15) Peinetti, A. S.; Lake, R. J.; Cong, W.; Cooper, L.; Wu, Y.; Ma, Y.; Pawel, G. T.; Toimil-Molares, M. E.; Trautmann, C.; Rong, L. Direct detection of human adenovirus or SARS-CoV-2 with ability to inform infectivity using DNA aptamer-nanopore sensors. *Sci. Adv.* **2021**, *7* (39), No. eabh2848.
(16) Zhang, L.; Fang, X.; Liu, X.; Ou, H.; Zhang, H.; Wang, J.; Li, Q.; Cheng, H.; Zhang, W.; Luo, Z. Discovery of sandwich type COVID-19 nucleocapsid protein DNA aptamers. *Chem. Commun.* **2020**, *56* (70), 10235−10238.
(17) (a) Song, Y.; Song, J.; Wei, X.; Huang, M.; Sun, M.; Zhu, L.; Lin, B.; Shen, H.; Zhu, Z.; Yang, C. Discovery of aptamers targeting the receptor-binding domain of the SARS-CoV-2 spike glycoprotein. *Anal. Chem.* **2020**, *92* (14), 9895−9900. (b) Deng, J.; Tian, F.; Liu, C.; Liu, Y.; Zhao, S.; Fu, T.; Sun, J.; Tan, W. Rapid One-Step Detection of Viral Particles Using an Aptamer-Based Thermophoretic Assay. *J. Am. Chem. Soc.* **2021**, *143* (19), 7261−7266.
(18) Broughton, J. P.; Deng, X.; Yu, G.; Fasching, C. L.; Servellita, V.; Singh, J.; Miao, X.; Streithorst, J. A.; Granados, A.; Sotomayor-Gonzalez, A. CRISPR−Cas12-based detection of SARS-CoV-2. *Nat. Biotechnol.* **2020**, *38* (7), 870−874.
(19) To, K. K.-W.; Tsang, O. T.-Y.; Leung, W.-S.; Tam, A. R.; Wu, T.-C.; Lung, D. C.; Yip, C. C.-Y.; Cai, J.-P.; Chan, J. M.-C.; Chik, T. S.-H. Temporal profiles of viral load in posterior oropharyngeal saliva samples and serum antibody responses during infection by SARS-CoV-2: an observational cohort study. *Lancet Infect. Dis.* **2020**, *20* (5), 565−574.
(20) Thi, V. L. D.; Herbst, K.; Boerner, K.; Meurer, M.; Kremer, L. P.; Kirrmaier, D.; Freistaedter, A.; Papagiannidis, D.; Galmozzi, C.; Stanifer, M. L.; Boulant, S.; Klein, S.; Chlanda, P.; Khalid, D.; Miranda, I. B.; Schnitzler, P.; Kräusslich, H.-G.; Knop, M.; Anders, S. A colorimetric RT-LAMP assay and LAMP-sequencing for detecting SARS-CoV-2 RNA in clinical samples. *Science translational medicine* **2020**, *12* (556), No. eabc7075.

https://doi.org/10.1021/jacs.1c09579
J. Am. Chem. Soc. XXXX, XXX, XXX−XXX